Electron emission from carbon foils induced by keV ions

S. M. Ritzau and R. A. Baragiola

Laboratory for Atomic and Surface Physics, University of Virginia, Thornton Hall, Charlottesville, Virginia 22903

(Received 12 February 1998)

We have measured yields of electrons emitted in the forward and backward directions from ultrathin carbon foils due to 10–100 keV atomic and molecular projectiles. In general, electron yields are higher in the forward than in the backward direction. Their behavior with projectile type and energy can be explained by a competition of a forward peaked angular distribution of initial ionization events and elastic collisions that tend to randomize electron motion in the foil. Experiments with ions with atomic number $Z = 1 - 10$ indicate that heavy projectiles produce less electron emission per amount of deposited energy by the projectile near the surface. This is attributed to a larger fraction of low-energy electrons produced by heavy projectiles in the primary ionization event that cannot surmount the surface barrier. For incident molecules, the backward electron yield is less than the sum of the yields of the constituent atoms. Neutral atoms with relatively low ionization potentials produce higher electron yields in the backward direction than the ions of the same species for incident energies above about 5 keV/amu, which is attributed to electron loss from the projectile. [S0163-1829(98)07629-2]

I. INTRODUCTION

When ionizing particles interact with solids, they excite electrons that can reach a surface and be emitted. The study of this phenomenon is motivated by the information it carries about the solid itself and the inelastic collisions within it. Furthermore, secondary electron emission is of great practical importance as a means of detecting the ionizing particle and its properties.[1–3] Fast atomic projectiles produce ionizations in solids mainly by nonadiabatic perturbations during collisions induced by the particle motion,[4,5] rather than by the potential energy they may carry that can be released by an Auger electron emission process[6] or plasmon excitation and decay.[7] In this kinetic electron emission the *primary* particle, the ionizing projectile, frees *secondary* electrons in collision events. These electrons then undergo a cascade of collisions in the solid, which can produce additional ionizations, until their energy degrades into heat or is stored in long-lived excited states. Those excited electrons that are energetic enough to be above the vacuum level and that are directed towards the surface of the solid may exit the solid before being thermalized, giving rise to secondary electron emission.

A common observable in electron emission is the average electron yield γ (number of electrons ejected per primary particle) either as an integral quantity or as a differential yield based on energy, angle of emission, and spin state. Electron emission events are statistically distributed; i.e., the yield fluctuates around the mean value γ and is described by probabilities of emission of n electrons per projectile. Generally, electron yields correlate in first order with the electronic stopping power $S_e = (dE/dx)$, at the surface, where dE is the energy loss spent in electronic processes per unit path length dx. Typically, ejected electrons have a most probable energy of a few eV and are emitted with a cosine angular distribution relative to the surface normal. This distribution is distorted if the Coulomb field of an ionic projectile is present.[8]

Of particular importance is electron emission from thin foils that is applied in time-of-flight mass spectrometers used in space applications,[9–11] and in backscattering spectroscopy for surface analysis.[12,13] For instance, in the ion mass spectrometer on NASA's Cassini mission to Saturn,[10,11] ions traverse an ultrathin carbon foil and the electrons they eject are used to provide a start pulse for a time-of-flight (TOF) measurement. Ion mass is derived using a speed measurement in conjunction with energy per charge analysis. In this instrument the highest mass resolution is obtained using the thinnest foils in order to minimize the angular and energy straggling the ions experience when passing through the foil. The Cassini instrument uses ultrathin carbon foils which are nominally $0.5~\mu g/cm^2$ (~ 25 Å) thick. In our work, connected with the data needs for the Cassini mission, we are interested in the physics of electron emission from foils, for instance, how the electron yields depend on the atomic number of the projectile, its energy, its charge state, and its state of aggregation (atoms vs molecules).

Previous studies using foil targets have concentrated on the higher electron yields that are often observed in the forward (downstream) direction compared to the yields in the backward direction.[14,15] This forward enhancement is normally attributed to an anisotropy in the angular distribution of electrons excited in individual atomic collisions between the projectile and an electron inside the foil. The literature shows large discrepancies not only in the values of the yields but also in their energy dependence.

II. EXPERIMENTAL TECHNIQUES

The experiments were performed in an ultrahigh vacuum chamber (base pressure in the 10^{-9} T range) connected to the University of Virginia 120-kV heavy ion accelerator, which provided a mass analyzed ion beam collimated to a diameter of 1 mm. The apparatus used to measure electron yields is shown schematically in Fig. 1. It was comprised of a foil holder, electrodes to measure electron and ion currents,
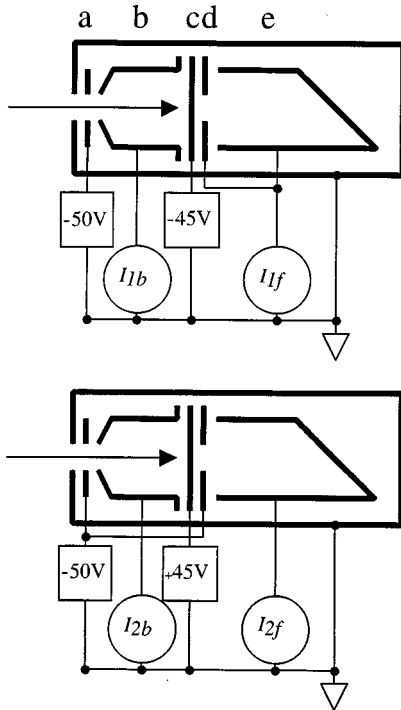
FIG. 1. Schematic diagram of experimental setup showing electron collection (top) and suppression (bottom) modes: The apparatus consists of carbon foil (c) surrounded by a backward electrode (a) and suppressor (b) and a forward Faraday cup (e) and electrode (f). The ion beam was measured in a movable upstream Faraday cup.

and electrodes to suppress secondary electrons from apertures. The foil divided the apparatus into upstream and downstream electrodes.

The incident beam current (I_{beam}) was measured in a movable upstream Faraday cup. Two additional current measurements were made to determine the electron yields. For the first measurement, all of the downstream electrodes were connected electrically and the foil was biased negative (-50 V) to accelerate secondary electrons toward the forward and backward electrodes. Ignoring pinholes and backscattered ions, which affect measurements by less than 1%, the current in the upstream collector is $I_{1b} = -\gamma_b I_{beam}$ and the current in the downstream Faraday cup is $I_{1f} = T(\Sigma_q f_q - \gamma_f) I_{beam}$. Here T is the transmission of the grid, and f_q are the fractions of the transmitted projectiles that have charge q. Values of $\Sigma_q f_q$ were obtained from measurements of charge distributions of ions through carbon foils performed at this laboratory[16] and elsewhere.[17,18] For the second measurement, the foil was biased positive ($+50$ V) to suppress electrons (return them back into the foil.) The forward suppressor was disconnected from the forward Faraday cup and biased at -50 V to prevent escape of secondary electrons from the back of this Faraday cup. In this configuration $I_{2b} = 0$ and $I_{2f} = T\Sigma_q f_q I_{beam}$. Leakage currents were limited to <1 pA, or $<0.2\%$ of measured currents. The backward and forward electron yields are then given by

$$\gamma_b = -I_{1b}/I_{beam}, \tag{1}$$

$$\gamma_f = (I_{2f} - I_{1f})/(T I_{beam}). \tag{2}$$

The ratio of the forward and backward yields is

$$R \equiv \gamma_f / \gamma_b = (I_{2f} - I_{1f})/(T I_{1b}). \tag{3}$$

This ratio is not subject to variations in the beam current and so can be measured more accurately. It can also be measured directly when using neutral beams, which cannot be measured directly in the Faraday cup. For neutral beams, the intensity can be obtained from the ratio $I_{2f}/[T(\Sigma_q f_q)]$ using the same ion fractions f_q as for incident ions, since the charge fractions are equilibrium values that do not depend on the charge of the ion entering the foil.[19] To obtain neutral beams, we passed the mass analyzed ion beam through a part of the beam line partially filled with a slight overpressure ($\sim 3 \times 10^{-5}$ T) of N_2 gas. A fraction of the beam was neutralized and the remaining ions were removed electrostatically. We were unable to measure the excitation state of the resulting neutrals, but we expect that the vast majority of those excited upon collisions with the gas will rapidly decay to the ground state, with only a few percent of long-lived metastable atoms remaining when the beam strikes the foil.[20]

The thin carbon foils used were manufactured by the Arizona Foil Co. They were floated in water, and mounted on $\sim 65\%$ transparency flat nickel grids[21] since they are too thin to be free standing. These foils, nominally 0.5 μg/cm^2, were found to be 1.4 μg/cm^2 from multiple-scattering experiments with protons.[22] The density of the foils $\rho = 1.8$ g/cm^3 was determined from the plasmon loss in electron-energy-loss spectrometry using the relationships given by Cuomo.[23] From this value and the mass per unit area, the thicknesses of the foils were found to be ~ 75Å The grid transparency, which was found to vary considerably among grids, was determined by measuring the mesh geometry using an optical microscope and from an absolute transmission measurement of an ion beam. For our measurements, the fraction of open area due to pinholes $\mathcal{A}$ acts to reduce the measured forward and backward electron yields by a factor of $(1 - \mathcal{A})$, while the ratio of forward to backward electron yield R is not affected by pinholes. The fraction $\mathcal{A}$ was measured to be <0.05 for all foils using a combination of current measurements and charge fraction data.

During preliminary measurements, we found that γ_f increased with ion bombardment before reaching a saturation value at ion beam fluences of $\sim 10^{16}$ ions/cm^2 that was 20–40 % higher than the initial γ_f. The backward electron yield was observed to be independent of the ion-beam fluence. Figure 2 shows an example of the measurement of the fluence dependence of R. A *decrease* in the electron yields with increasing fluence has been observed in the past using MeV multiply charged ions on thicker foils. Arrale *et al.*[24] found a decrease of up to 16% in the total electron yield ($\gamma_f + \gamma_b$) from 50 μg/cm^2 foils after irradiation with $\sim 4 \times 10^{15}$ F$^+$/cm^2 at 4 MeV, which they attributed to desorption of surface contaminants which decreased the work function of the foil. Rothard *et al.*[25] measured a 14–36 % decrease in the total electron yield from 10 μg/cm^2 foils after irradiation with $\sim 10^{15}$ ions/cm^2 of ~ 10 MeV/u heavy ions, and attributed the change to surface smoothing and desorption processes at the surfaces of the foil induced by electronic transitions.
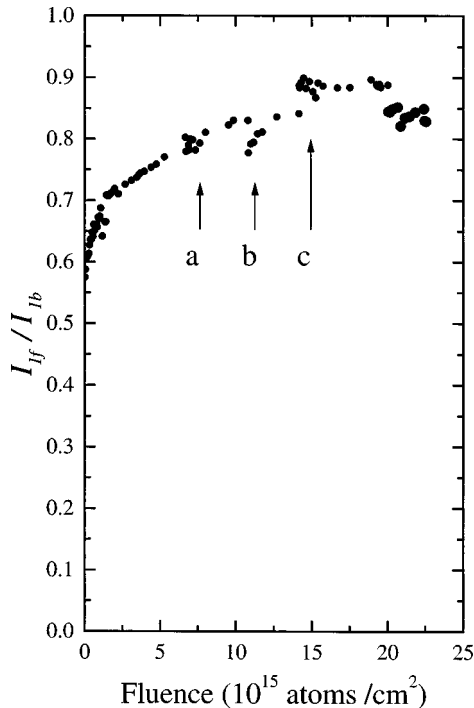
FIG. 2. Ratio of forward to backward currents (I_{1f}/I_{1b}) from a 0.5 μg/cm^2 carbon foil as a function of fluence under 30 keV H_2^+ ion bombardment, measured with the foil biased negative. The arrows on the graph indicate when (a) bombardment was ceased for 15 min and then resumed; (b) the bias on the foil was changed from negative to positive and then changed back; and (c) the chamber was vented to dry nitrogen, left at atmospheric pressure for 2 h, re-evacuated, and bombardment was resumed.

We attribute the increases in the forward yield in our experiments to the removal of contaminants by sputtering, since the forward side of the foil was adjacent to the parting agent that enables separation of the foil from the glass slide on which it was grown during manufacture. The initially smaller yields suggest the emission of positive ions or that the contaminant layer has a lower electron yield than carbon, a high yield material. Using x-ray photoelectron spectroscopy we found Na contaminants, which usually desorb as Na$^+$,[26] on the surface of untreated foils. We note that, unlike the MeV experiments,[24,25] sputtering in our case is not only by electronic but also by knock-on processes and, therefore, more effective in desorbing strongly bound contaminants such as Na. We notice that the cleaning process is irreversible, since after we do it, we obtain reproducible yields even after briefly exposing the ''cleaned'' foils to the atmosphere. The results presented below were determined using foils irradiated well past saturation fluences.

III. EXPERIMENTAL RESULTS

Figure 3 shows electron yields in the forward and backward direction for protons incident on 0.5 μg/cm^2 foils, together with results of other studies. We used deuterons to extend the range to lower velocities since there is no isotope effect when comparing yields for protons and deuterons at the same velocity.[27] The results of Meckbach *et al.* for 5 and 10 μg/cm^2 foils[15] agree roughly at high energies but their data appears too high at low energies and do not follow the
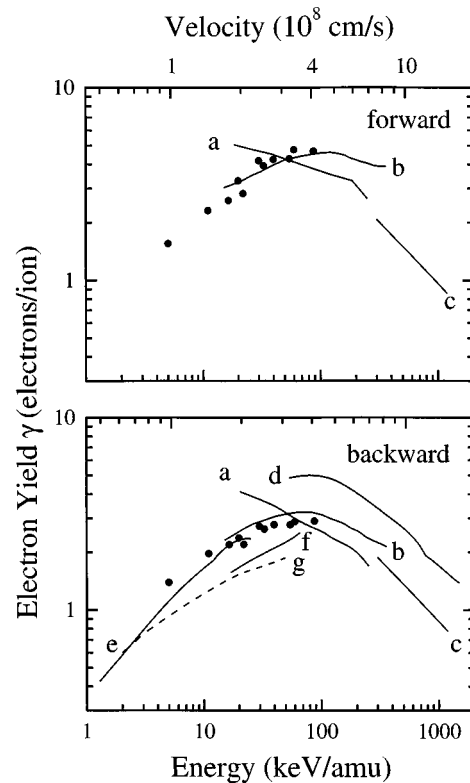
FIG. 3. Electron yields for incident protons. Measured electron yields in the forward (exit) and backward (entrance) directions for H$^+$ incident on 0.5 μg/cm^2 foils (●). Also shown are the results of (a) Meckbach *et al.* (Ref. 15) for 5 and 10 μg/cm^2 foils, (b) Rothard *et al.* (Ref. 33) for sputter-cleaned 10 μg/cm^2 foils, (c) Gelfort *et al.* (Ref. 34) for 3 μg/cm^2 foils, (d) Billebaud *et al.* (Ref. 32) for sputter-cleaned 7 μg/cm^2 foils, (e) Likhtenshtein and Tankov (Ref. 29) for 1.0 μg/cm^2 foils. The data by (g) Large and Whitlock (Ref. 35) and (f) Alonso *et al.* (Ref. 36) are for bulk carbon samples.

trend expected from stopping powers at low energies.[28] Based on our data for molecular ions presented below, we suspect that an explanation for the strong deviation at the lowest energies may be that these authors inadvertently used H$_2^+$ instead of H$^+$ beams at their lowest energies. Our data agree fairly well with that of Likhtenshtein and Tankov[29] for 1.0 μg/cm^2 carbon foils. The results of Gruntman, Kozochkina, and Leonas[30] and Leonas[31] on 1 μg/cm^2 foils is a factor of 2–3 lower than the data from this and other papers, and are not shown in the figure. The data of Billebaud *et al.*[32] for the backward yield from 10 μg/cm^2 foils lies about 15% higher than our results and also lies above the high-energy data of Rothard *et al.*[33] for sputter cleaned 10 μg/cm^2 foils. There is in general a good agreement with the recent results by Gelfort *et al.*[34] on ~3 μg/cm^2 foils. Also shown in Fig. 3 are backward electron yield data obtained from bulk graphite targets,[35,36] which are about 30% lower than the foil results.

To test for differences in excitation processes between light and heavy projectiles, we measured electron yields for all elements from H to Ne. The results, presented in Fig. 4, show two general trends: for a given velocity, the yields increase with increasing atomic number of the projectile and for each species the yields vary with velocity v as v^m, with m close to unity. For proton impact, a deviation from this
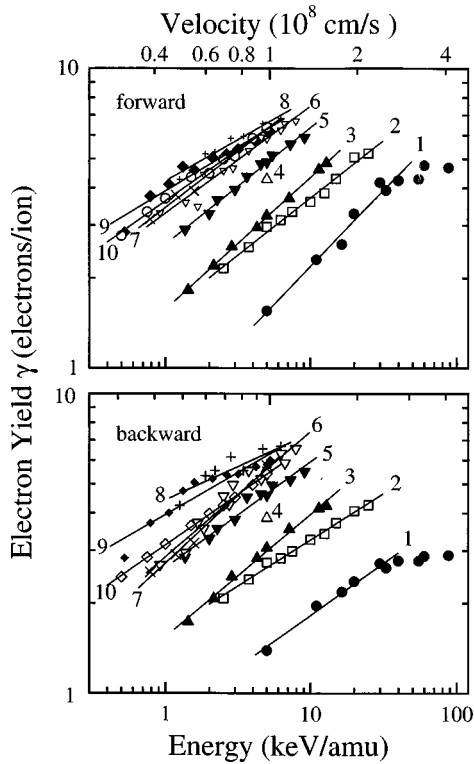
FIG. 4. Electron yields for ions of atomic number $Z = 1 - 10$ as a function of velocity or energy/mass. The lines indicate a dependence $\gamma \sim v^m$. They are labeled by the atomic number of the projectile.

behavior at high v follows an analogous trend in the electronic stopping power.

The directly measured ratio between the forward and backward yields $R = \gamma_f / \gamma_b$, is shown in Fig. 5 as a function of incident velocity v. For all projectiles R increases with v starting with a value near unity at low v. A value lower than one is expected at low energies if the ions in the foils are sufficiently thick to slow down the projectiles significantly. This behavior is seen in the data of Likhtenshtein, Shabelni-kova, and Yasnoposky[37] suggesting that the thickness given by the authors ($0.8 \, \mu\text{g cm}^2$) is a nominal value quite lower than the real value, as found in our work. A larger forward than backward yield at high v is expected from the forward peaked distribution of electrons from primary ionization events.[14,38]

The ratio of the electron yields to the stopping power, γ/S_e, derived using S_e measured by Ormrod and Duckworth,[56] is shown in Fig. 6. It can be seen that the proportionality of γ with S_e is only valid within about 30% for different projectiles and velocities. For forward emission γ/S_e increases with v for protons and is nearly constant for heavy ions in our measured velocity range; we note that γ/S decreases with v at high velocities from the yields reported by Keller et al.[57] for C and Ne projectiles. For backward emission, γ/S_e is either constant or decreases slightly at high v.

The variation of the electron yields with the atomic number of the projectile Z is shown in Fig. 7 at a constant velocity corresponding to 5 keV/amu. The yields $\gamma(Z)$ show a much weaker structure than the strong Z oscillations in S_e, an effect reported by Alonso, Baragiola, and Oliva-Florio.[36]
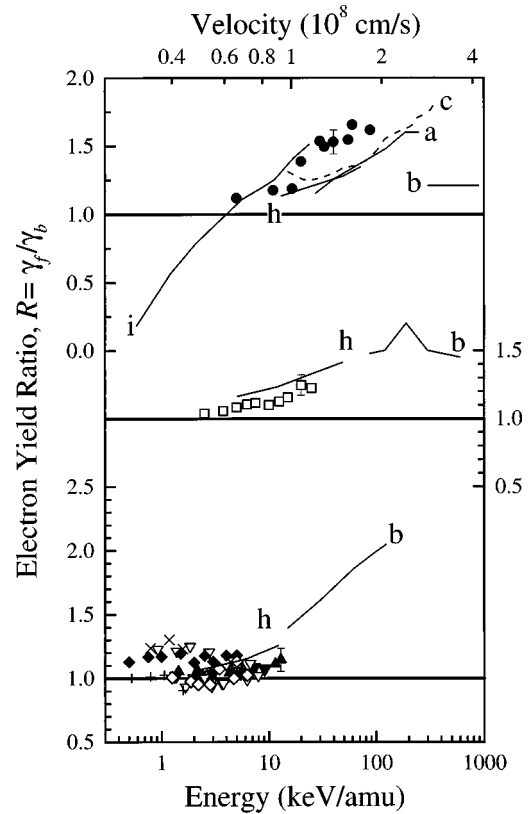

FIG. 5. Ratio of forward to backward yields. Top: Results for hydrogen (●) shown with the results of (a) Meckbach et al. (Ref. 15) for 5 and 10 $\mu\text{g/cm}^2$ foils, (b) Rothard et al. (Ref. 33) for sputter-cleaned 10 $\mu\text{g/cm}^2$ foils, (c) Gelfort et al. (Ref. 34) on 3 $\mu\text{g/cm}^2$ foils, (h) Gruntman et al. (Ref. 30), and, (i) Likhtenshtein and Shabelnikova (Ref. 37) on 0.8 $\mu\text{g/cm}^2$ foils. Center: Results for helium (□) along with results of (b) Rothard et al. (Ref. 33) and (h) Gruntman et al. (Ref. 30). Bottom: Results for ions $Z = 3 - 10$ (▲ Li, △ Be, ▼ B, ▽ C, × N, + O, ◆ F, ◇ Ne) with results of (b) Rothard et al. (Ref. 33) for Ne and (h) Gruntman et al. (Ref. 30) for O. Error bars are shown at representative points.

Also shown in Fig. 7 is a remarkable decrease of the γ/S_e ratio when going from H to B, followed by a relatively constant value for the heavier elements.

An interesting question is how the electron yields produced by molecular ions compare to the yields produced by their constituent atoms. For hydrogen projectiles on clean metals, previous studies indicate that the ratio of the yields $\gamma(H_2^+, v)/2\gamma(H^+, v)$ at equal velocity is less than one below $\sim 4.5 \times 10^8$ cm/s and larger than one at higher velocities.[2,39–42] The reduction at low velocities occurs even taking into account a smaller potential electron emission yield by molecular ions.[6] A similar effect has been observed for hydrogen clusters traversing thicker ($\geq 7.2 \, \mu\text{g/cm}^2$) carbon foils at energies above 40 keV/amu by Rothard et al.[43]

Figure 8 shows our secondary electron measurements for H_2^+ projectiles. These results show that $\gamma_m < \Sigma \gamma_i$ down to 10 keV/amu indicating a molecular effect in the secondary electron yields in the backward direction. A similar, although weaker, effect is observed for forward emission.

To determine if a molecular effect exists also for heavy ions and if it is the same for forward and backward emission, we did experiments with a range of homonuclear and hetero-
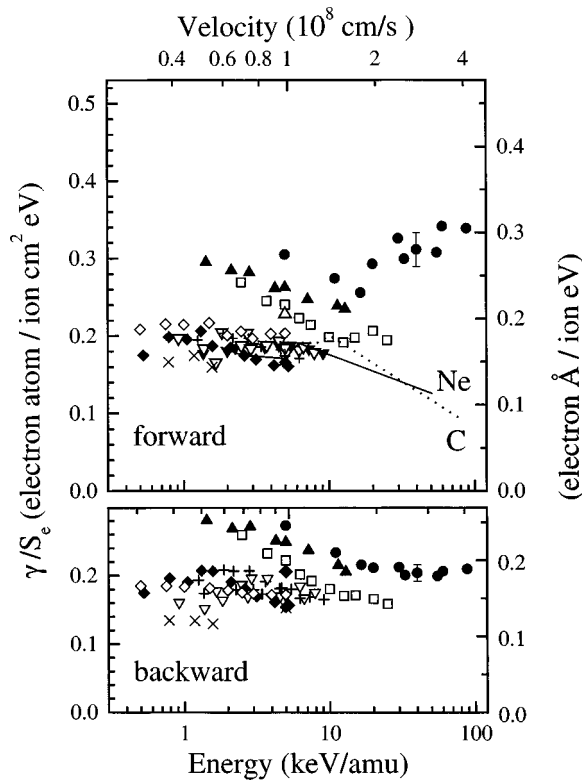
FIG. 6. Electron yields divided by electronic stopping power for incident ions $Z=1-10$ (● H, □ He, ▲ Li, △ Be, ▼ B, ▽ C, × N, + O, ◆ F, ◇ Ne). Stopping power values were obtained by interpolating the values measured by Ormrod *et al.* (Ref. 56) and were converted from eV cm^2/atom to eV/Å using a measured density of 1.8 g/cm^3. Also shown are the data of Keller *et al.* (Ref. 57) (lines) for Ne and C. Data by Keller *et al.* (Ref. 57) for incident N and O (not shown) agree with our values within 5%. Typical error bars are shown at representative points.
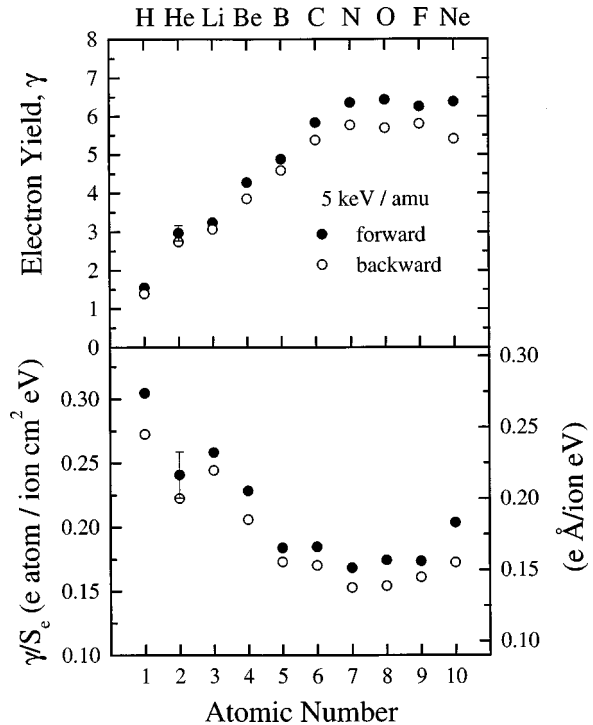

FIG. 7. Electron yields (top) and ratio of electron yields to electronic stopping power (bottom) as a function of the atomic number of the projectile at 5 keV/amu ($v=9.6\times10^7$ cm/s). Stopping power values were obtained by interpolating the values measured by Ormrod *et al.* (Ref. 56) and were converted from eV cm^2/atom to eV/Å using a measured density of 1.8 g/cm^3.

nuclear molecular projectiles. We compare the electron yield for the incident molecular ion γ_m to the sum of the electron yields of its constituent atoms $\Sigma\gamma_i$. If the yields are additive ($\gamma_m=\Sigma\gamma_i$), the ratio $\gamma_m/\Sigma\gamma_i$ should be unity. As a corollary, the yield of a constituent atom could be obtained by subtracting all the other γ_i from the molecular yield. In the case of most heavy molecular projectiles no molecular effect is observed, within error, for the forward yields which are seen to be additive in this energy range. For backward yields, $\gamma_m<\Sigma\gamma_i$.

A long-standing question of great practical importance for detecting energetic neutral atoms has been whether fast neutrals produce the same or different kinetic electron emission yields than the corresponding ionized projectiles (ions produce more *potential* electron emission than ground-state neutrals if they have sufficiently high potential energy.) Because the intensity of the incident neutral beam cannot be measured directly in the Faraday cup, we measured $I_{2f}=T\Sigma_q f_q I_{beam}$ and I_{beam} for incident ions and determined the neutral beam intensity from I_{2f} using the fact that the charge-state distribution ($\Sigma_q f_q$) of the beam after traversing the foil is independent of the incoming charge state. The results shown in Fig. 9, indicate that the backward yields for neutral atoms are either larger or nearly equal to the yields for positive ions. To clarify the contribution of the kinetic electron emission,

the potential emission was subtracted from the measured yields using an empirical expression.[44]

Figure 10 shows that the backward electron yields for fast H, Li, and C are higher for incident neutrals than for ions. We found no significant difference in the yields for ions and neutrals of fast He, O, and F, all of which have relatively high ionization potentials. We also saw no effect of the in-
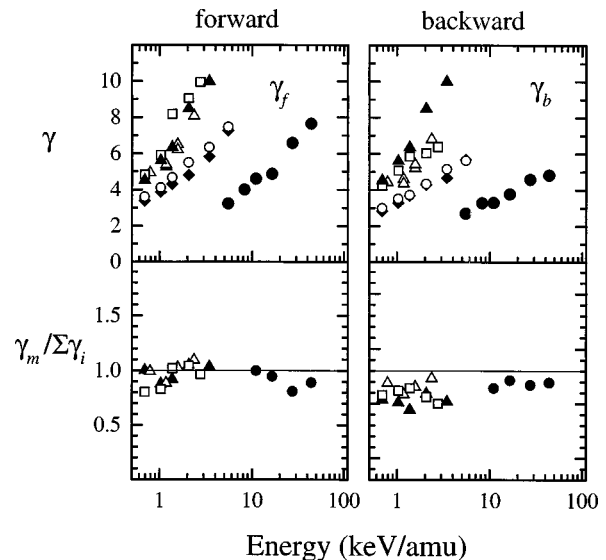

FIG. 8. Electron yields for incident molecules including: (top) electron yields for molecular ions and (bottom) additivity of molecular yields. (● H$_2$, ◆ OH, ○ H$_2$O, ▲ CO, △ N$_2$, □ O$_2$).
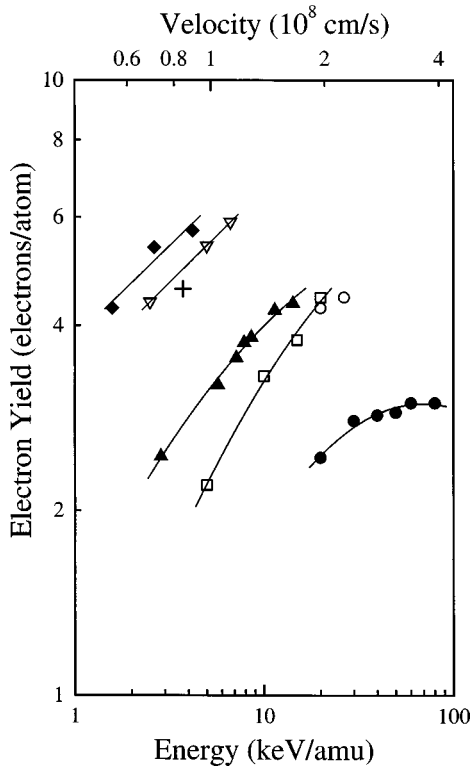
FIG. 9. Backward electron yields for incident neutral atoms (● H, □ ³He⁺, ○ ³He⁺⁺, ▲ Li, + + O, ◆ F).

cident charge state on kinetic electron emission for $^3\text{He}^{++}$ compared to $^3\text{He}^+$ in the energy range used here, where kinetic yields are again obtained by subtracting potential emission yields in both cases.[45]

IV. DISCUSSION

To discuss the results we need to recall the main picture of electron emission from solids induced by heavy particles,[4] which can be understood as follows: the projectile frees and energizes secondary electrons in the solid in collisional ionization events. These energetic electrons then undergo a cascade of collisions with other electrons in the solid, which can produce additional ionization, until their energy degrades into heat or is stored in long-lived excited states. Those excited electrons that are directed towards the surface can cross the surface of the solid and escape, giving rise to electron emission. We concentrate here on kinetic electron emission where the electrons are excited by the time-dependent perturbation set up by the projectile. This is the dominant mechanism in our experiments, since potential electron emission due to neutralization by the Auger effect[6] or accompanied by plasmon excitation[46] are expected to be significant only at the entrance surface of the foil and for projectiles having a high first ionization potential energy, like He⁺, F⁺, and Ne⁺. In these cases, potential electron yields can be estimated to be 0.3, 0.11, and 0.22, respectively, and are expected to be roughly independent of velocity below 10^8 cm/s.[6] Potential emission from the downstream surface of the foil should not be important since projectiles exit mainly as ground-state neutral atoms.

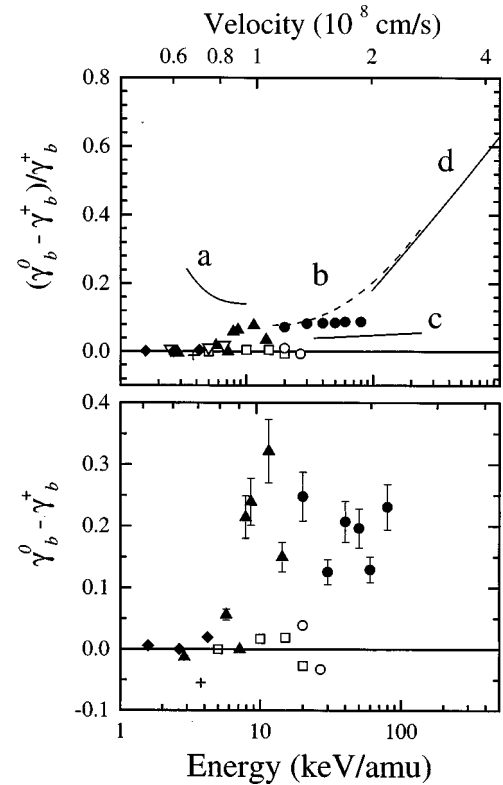An ionization event can free an electron directly from the

FIG. 10. Relative enhancement in the backward-directed electron yields of incident neutrals with respect to incident singly charged ions at the same velocity (top) and difference in the yields (bottom) for (● H, □ ³He⁺, ○ ³He⁺⁺, ▲ Li, + O, ◆ F.) Also shown are the proton data of (a) Bethge and Lexa (Ref. 69) for Li incident on beryllium, of Stier *et al.* (Ref. 70) for H (b) and He (c) on a nickel foil and (d) Barnett and Reynolds (Ref. 71) for a brass target. The quantity $\gamma_b^0 - \gamma_b^+$ for (a)–(d) is out of range in the lower figure. For positive values, the difference $\gamma_b^0 - \gamma_b^+$ can be interpreted as the probability of electron loss from the projectile into vacuum. The contribution to the yields due to potential electron emission has been subtracted using the expression of Baragiola *et al.* (Ref. 44).

projectile or a target atom, indirectly through inner shell excitations followed by Auger decay, or by decay of plasmon excitations in the carbon valence band. From measurements in gas-phase collisions,[47,48] the angular distribution of electrons from direct ionizations is expected to be forward peaked, especially for the more energetic excited electrons. The energy distributions of electrons in single gas-phase collisions at the impact velocities considered here are of the form $N(E) \propto \exp(-E/b)$ for light ions[49] and $N(E) \propto E^{-1}\exp(-E/(bv))$ for impact of multielectron ions,[50] where E is the electron energy and b is a constant. That is, heavy projectiles produce an energy distribution which is ''softer'' (with a lower mean energy) compared to that produced by light projectiles. Other inelastic processes that can lead to electron emission are inner-shell excitations, which are very unlikely in carbon at the energies used in this work but may occur in the L shell of lighter projectiles. Plasmons can be excited kinetically in the foils by projectiles faster than about 5 keV/amu.[2,51] Excited electrons can produce additional ionizations in a cascade of ionizing collisions if their energy is sufficiently high. This cascade multiplication factor

increases with projectile velocity and is expected to be about two for 100 keV protons.[4] Excited electrons can also scatter elastically from target atoms with a mean free path between collisions that increases with increasing electron energy.[52] These elastic collisions can involve large deflection angles and thus tend to make the initially forward peaked distribution of excited electrons isotropic. If excited electrons lose enough energy in an inelastic collision to drop below the vacuum level of the solid they cannot be ejected. This leads to an escape depth from which electrons can originate. Its magnitude decreases with electron energy up to about 100 eV, which covers the vast majority of energies of ejected electrons.[15] The mean value of the escape depth of secondary electrons in carbon is about 30 Å,[53] smaller than our foil thickness (~ 75 Å).

Relation of the electron yields with the electronic stopping power S_e

The number of electrons excited inside the carbon foil ν cannot be measured with our experimental techniques. By analogy to ionization processes in dense gases and semiconductor solids, ν is expected to be proportional to the electronic energy deposited in the foil and independent of the type of projectile to a first approximation.[27,47] Previous studies have implicitly assumed that the number of electrons emitted from the solid is also proportional to the electronic energy deposited. This leads to a general relationship[14,54,55]

$$\gamma = B S_e / \cos(\alpha) \qquad (4)$$

which has been found to hold reasonably well for many targets. Here, α is the incidence angle of the projectile relative to the surface normal (0 in our case). The factor B is relatively independent of the target material and depends on the depth distribution, the energy distribution, and the escape probability of the secondary electrons generated in the solid. The proportionality between γ and S_e is best tested with the aid of Fig. 6 where we plot the ratio γ/S_e, where γ are the measured electron yields and S_e is the electronic stopping power obtained by interpolation from the values measured by Ormrod and Duckworth.[56] The values of γ/S_e for backward emission are 2–3 times larger than for clean metals.[54]

Our results show that B is not constant, but varies with the type of projectile, being larger for the lighter ions (H, He, Li). B decreases with increasing incident velocity, more strongly for the lighter projectiles, except for the forward electron emission data for protons at velocities above 1.5×10^8 cm/s where B increases with velocity. The decrease of B with impact velocity, which has not been explained, has been seen previously for C, N, and O projectiles by Keller et al.[57] in our energy range, who found values similar to ours but in thicker foils (nominal 2.0 μg/cm^2). The upward trend of B at the highest velocities measured in this work for H and He is consistent with higher B values around 0.31 eV/Å that were found for the total yields ($\gamma_f + \gamma_b$) from carbon foils bombarded by faster ions ranging from hydrogen to uranium.[2,58,59] The near independence of γ/S_e on ion type in those studies contrasts with our finding of lower ratios for heavier ions, which is consistent with other low-energy results.[60,61]

The variation of B from carbon foils with the type and velocity of the ion implies the need to refine the assumptions that led to Eq. (4). It means that, unlike the total number of excited electrons ν, the number of those that can escape is not proportional to the stopping power. We note that the interpenetration of the electron clouds in heavy ion collisions leads to shell effects in the stopping power, seen in strong oscillations of S_e vs Z.[56,62] These Z oscillations are mainly caused by soft collisions which produce low-energy electrons which do not escape the solid, which explains the weaker structure seen in the $\gamma(Z)$ dependence of Fig. 7, an effect previously observed and discussed for thick Al targets.[60] This in turn implies that the shape of the low-energy part of the distribution of excited electrons (that contributing to most of the electron yield) is not constant, as would be the case if it were dominated by the cascade of electron collisions in the solid.[55,63] Therefore, the variation of B with the type and energy of the projectile implies that the shape of the energy distribution of electrons depends on these variables. The decrease of B with Z can be understood by noting that, as indicated above, the energy distribution of low-energy electrons in the primary ionization is softer for slow multielectron projectiles. This means that a larger proportion of these electrons will not be able to escape the solid, explaining the smaller electron yield per energy deposited for heavier projectiles seen in Fig. 5.

The larger proportion of excited electrons that cannot leave the solid in the case of heavy ion bombardment serves also to explain a long-standing puzzle, that keV heavy projectiles traversing thin carbon foils have an unusually large probability of not emitting any electron on impact even when the *mean* electron yields are high.[31,64] This property, which limits the efficiency of particle detectors based on secondary electron emission, explains the reduced usefulness of ultrathin carbon foils in low-velocity TOF spectrometers for ions[12,13] since ion detection requires that at least one electron be emitted from the foil.

Forward-backward ratios R

According to a high velocity model by Sternglass,[14] the ratio of forward-to-backward electron emission R should be larger than one, since the faster electrons produced in ionization events are ejected predominantly forward, along the direction of the projectile velocity. Such fast electrons will then tend to deposit their energy downstream from their point of creation thus exciting more electrons near the exit surface than near the entrance surface. The magnitude of this enhancement in the electron emission in the forward direction will decrease as a result of elastic collisions with target atoms that tend to reduce the anisotropy in the excitation source. The increase in the mean electron energy with increasing particle velocity[48,49] and the dominance of elastic scattering at low electron energies[52] serves to explain different observations: (i) the low value of R at low impact velocities due to a more isotropic distribution of electrons from the first ionization events and a lower mean energy of excited electrons and (ii) at a given impact velocity, R measured for specific energies of the emitted electrons increases with electron energy[15] due to an increase in the anisotropy of the ionization event and a decrease in the mean free path for elastic scattering.

We note several additional factors affect R, important only at low impact velocities, which have not been considered in earlier work concentrated on fast projectiles. Potential electron emission will produce $R<1$ for slow projectile ions that carry high potential energy. This is because potential emission due to Auger neutralization is more likely to occur at the entry surface than at the exit surface, where most of the projectiles exit as neutrals in the ground state and are therefore incapable of ejecting electrons by the potential mechanism. The fact that $R\sim1$ at low velocities indicates that potential emission is relatively unimportant in carbon even for projectiles of large potential energy, like He^+ and Ne^+.

Multiple scattering of the projectiles will produce longer trajectories over the escape depth from the exit surface and, hence, more energy deposition there. For thicker foils, where this effect is important, it will be counterbalanced by a decrease in the projectile energy, which is accompanied by a smaller electronic stopping power. An enhanced forward electron emission yield will also result from the electronic energy deposited by recoiling target atoms set in motion preferentially in the forward direction by close collisions with the projectile. This recoil effect[6] should increase with the cross section for scattering between the projectile and the target atom and, hence, with the atomic number of the projectile. This effect may be important at low energies for the heavier ions used in this work, based on estimates using the TRIM Monte Carlo simulation code,[65] but these simulations have large uncertainties in the electronic stopping power of the slow recoil ions.

Molecular effects

The fact that projectile atoms eject less electrons when they are aggregated in molecules is most likely related to a similar effect in S_e of hydrogen molecules: molecular ions lose less energy than protons at low velocities and more at high velocities. This has been explained as resulting from an interference in the scattering of the target electrons in the molecular centers.[66] At high velocities where the dynamic screening is weakened, the two protons act like a He^{2+} ion in distant collisions and give a higher yield due to the Z^2 dependence of S_e. Additional emission may also result from loss of the electron carried by the H_2^+ ion.

The absence of a molecular effect in the forward yields for slow heavy ions can be explained from the effect of strong multiple scattering in addition to the screened Coulomb repulsion between fragments which take place after the molecules dissociate in the first few layers of the foil. These effects separate the fragments so they behave like independent particles during their transit through the foil.

Electron emission by neutral projectiles

Two arguments have been proposed to explain or predict differences in the electron yields for neutrals and singly charged ions. The electron yield γ for neutrals may be smaller due to a presumably lower S_e for neutrals than for ions or it may be larger due to the additional electron emission resulting from electron loss by the projectile. Compar-

ing atomic projectiles with similar stopping power but widely different ionization potentials can test the second hypothesis.

We find that an enhancement in the backward yield is observed for the projectiles with lower ionization potential, suggesting the importance of electron loss from the projectile in these cases. The fact that we do not observe the increased yields for $^3He^{++}$ compared to $^3He^+$ that have been seen at higher velocities[67,68] is attributed to a very fast charge equilibration of the incident projectile in the surface layers due to large electron capture and loss cross sections.[20] Thus, even though one would expect a projectile charge dependence in the stopping powers, this fast charge equilibration by collisions (which include electron transfer outside the surface) acts to suppress a dependence of the kinetic electron yield on the charge of the projectile. We notice in Fig. 10 that there appears to be a velocity threshold for electron loss from the projectile, at around $0.9-1.4\times10^8$ cm/s, which corresponds to the velocity of an incoming electron with a kinetic energy of $2-5$ eV. We note that at high velocities the difference in the yields can be larger than one if the electron detached from the projectile is energetic enough to eject additional electrons from the solid.

V. CONCLUSIONS

We have studied the emission of electrons from both the entrance and exit surfaces of ultrathin carbon foils traversed by $Z=1-10$ ions in the energy range $10-100$ keV. Deviations from the proportionality of electron yields to the stopping power of the projectile are explained as changes in the fraction of excited electrons that can leave the foil, due to changes in the energy distribution of electrons in the primary ionization event. This implies that the electron energy distributions are not dominated by the cascade of collisions that electrons undergo before escaping the solid. According to this picture, heavier ions produce a larger fraction of low-energy electrons which cannot escape the solid, and therefore a lower electron yield per amount of energy deposited over the electron escape depth, compared to light projectiles.

The ratio of forward-to-backward electron yields is close to 1 at low velocities and increases steeply above $\sim8\times10^7$ cm/s. This is explained by an increasing mean energy of the excited electrons and the accompanying decrease in importance of elastic electron scattering which enables the excited electrons to retain part of the forward peaked distribution of the initial ionization event. The energy dependence of the forward-to-backward ratio is more pronounced for lighter ions due to a larger mean electron energy in the primary ionization collisions.

A molecular ion produces a smaller yield of electrons in the backward direction than the sum of the yields produced by its constituent atoms. This is related to observed nonlinear effects in the energy deposited by molecules. The molecular effect disappears in the forward direction due to the dissociation of the molecule upon entry to the foil and the quick separation of the resulting fragments by mutual repulsion and multiple scattering, which cause them to act independently.

Kinetic electron yields for neutral atoms are the same as those for ions at low velocities but become larger at velocities above 0.9–1.4×10^8 cm/s for atoms of low ionization energy. We attribute this behavior to electron loss from the projectile followed by scattering into vacuum.

[1] L. N. Dobretsov and M. V. Gomoyunova, *Emission Electronics* (Israel Pro. Sci. Trans., Jerusalem, 1971).

[2] D. Hasselkamp, H. Rothard, K.-O. Groeneveld, J. Kemmler, P. Varga, and H. Winter, *Particle Induced Electron Emission II* (Springer-Verlag, Berlin, 1992).

[3] *Ionization of Solids by Heavy Particles*, edited by R. A. Baragiola (Plenum, New York, 1993).

[4] R. A. Baragiola, Nucl. Instrum. Methods Phys. Res. B **78**, 223 (1993), and references therein.

[5] H. Rothard, Scanning Microsc. **9**, 1 (1995).

[6] R. A. Baragiola, in *Low Energy Ion-Surface Interactions*, edited by J. W. Rabalais (Wiley, New York, 1994), Chap. 4.

[7] R. A. Baragiola and C. A. Dukes, Phys. Rev. Lett. **76**, 2547 (1996).

[8] W. Meckbach and R. A. Baragiola, in *Inelastic Ion-Surface Collisions* (Academic, New York, 1977), p. 283.

[9] B. Wilken, Rep. Prog. Phys. **47**, 767 (1984).

[10] D. T. Young *et al.*, Proc. SPIE **1803**, 118 (1996); D. J. McComas *et al.*, Proc. Natl. Acad. Sci. USA **87**, 5925 (1990).

[11] D. J. McComas and J. E. Nordholt, Rev. Sci. Instrum. **61**, 3095 (1990).

[12] M. H. Mendenhall and R. A. Weller, Nucl. Instrum. Methods Phys. Res. B **47**, 193 (1990).

[13] C. A. Dukes, M.S. thesis, University of Virginia, 1993.

[14] E. J. Sternglass, Phys. Rev. **108**, 1 (1957).

[15] W. Meckbach, G. Braunstein, and N. Arista, J. Phys. B **6**, L344 (1975).

[16] S. M. Ritzau, Ph.D. thesis, University of Virginia, 1997.

[17] A. Bürgi *et al.*, J. Appl. Phys. **68**, 2547 (1990); **73**, 4130 (1993).

[18] H. O. Funsten, B. L. Barraclough, and D. J. McComas, Nucl. Instrum. Methods Phys. Res. B **80/81**, 49 (1993).

[19] S. K. Allison and M. García-Muñoz, in *Atomic and Molecular Processes*, edited by D. R. Bates (Associated Press, New York, 1962).

[20] H. S. W. Massey and H. B. Gilbody, *Electronic and Ionic Impact Phenomena* (Oxford University Press, London, 1974), Vol. IV, Chap. 24.

[21] Supplied by Buckbee Mears St. Paul, St. Paul, Minnesota 55101.

[22] H. Funsten and M. Shapprio, Nucl. Instrum. Methods Phys. Res. B **127/128**, 905 (1997).

[23] J. J. Cuomo, J. P. Doyle, J. Bruley, and J. C. Lui, Appl. Phys. Lett. **58**, 1 (1991).

[24] A. M. Arrale *et al.*, Nucl. Instrum. Methods Phys. Res. B **89**, 437 (1994).

[25] H. Rothard, M. Jung, B. Gervais, J. P. Grandin, A. Billebaud, and R. Wuensch, Nucl. Instrum. Methods Phys. Res. B **107**, 108 (1996).

[26] A. Benninghoven, F. G. Rüdenauer, and H. W. Werner, *Secondary Ion Mass Spectrometry: Basic Concepts, Instrumental Aspects, Applications, and Trends* (Wiley, New York, 1987).

[27] R. A. Baragiola, E. V. Alonso, and A. Oliva-Florio, Phys. Rev. B **19**, 121 (1979).

[28] H. H. Andersen and J. F. Ziegler, *Hydrogen Stopping Powers and Ranges in All Elements* (Pergamon, New York, 1977).

[29] V. K. Likhtenshtein and I. I. Tankov, Sov. Tech. Phys. Lett. **1**, 424 (1975).

[30] M. A. Gruntman, A. A. Kozochkina, and V. B. Leonas, JETP Lett. **51**, 22 (1990).

[31] V. B. Leonas, Sov. Phys. Usp. **34**, 317 (1991).

[32] A. Billabaud *et al.*, Nucl. Instrum. Methods Phys. Res. B **98**, 496 (1995).

[33] H. Rothard *et al.*, Phys. Rev. A **41**, 2521 (1990).

[34] St. Gelfort, H. Kerkow, R. Stolle, V. P. Petukov, and E. A. Romanovskii, Nucl. Instrum. Methods Phys. Res. B **125**, 49 (1997).

[35] L. N. Large and W. S. Whitlock, Proc. Phys. Soc. London **79**, 148 (1962).

[36] E. V. Alonso, R. A. Baragiola, and A. Oliva-Florio (unpublished).

[37] V. Kh. Likhtenshtein, A. V. Shabelnikova, and K. K. Yasnoposky, Radiotekh. Elektron. **23**, 1251 (1978); E. S. Parilis *et al.*, *Atomic Collisions on Solid Surfaces* (North-Holland, Amsterdam, 1993).

[38] J. C. Dehaes and A. Dubus, Nucl. Instrum. Methods Phys. Res. B **78**, 255 (1993).

[39] R. Baragiola, E. Alonso, O. Auciello, J. Ferrón, G. Lantschner, and A. Oliva-Florio, Phys. Lett. **67A**, 211 (1978).

[40] N. R. Arista, M. M. Jakas, G. H. Lantschner, and J. C. Eckardt, Phys. Rev. A **34**, 5112 (1986).

[41] B. Svensson and G. Holméen, Phys. Rev. B **25**, 3056 (1982).

[42] D. Hasselkamp and A. Scharmann, Phys. Status Solidi A **79**, K197 (1983), and Ref. 3.

[43] H. Rothard, D. Dauvergne, M. Fallavier, K-O. Groeneveld, R. Kirsch, J-C. Poizat, J. Remillieux, and J-P. Thomas, Radiat. Eff. Defects Solids **126**, 373 (1993).

[44] R. A. Baragiola, E. V. Alonso, J. Ferrón, and A. Oliva Florio, Surf. Sci. **90**, 240 (1979).

[45] H. D. Hagstrum, in *Inelastic Ion Surface Collisions*, edited by N. H. Tolk, J. C. Tully, W. Heiland, and C. W. White (Academic, New York, 1977), p. 1.

[46] R. A. Baragiola and C. A. Dukes, Phys. Rev. Lett. **76**, 2547 (1996).

[47] L. H. Toburen, in *Atomic and Molecular Data for Radiotherapy and Radiation Research*, IAEA-TECDOC-799 (International Atomic Energy Agency, Vienna, 1995), Chap. 2.

[48] R. K. Cacak and T. Jorgensen, Phys. Rev. A **2**, 1322 (1970).

[49] M. E. Rudd, Y-K. Kim, D. H. Madison, and T. J. Gay, Rev. Mod. Phys. **64**, 441 (1992).

[50] P. H. Woerlee, Yu. S. Gordeev, H. de Waard, and F. W. Saris, J. Phys. B **14**, 527 (1981).

[51] S. M. Ritzau, R. A. Baragiola, and R. C. Monreal (unpublished).

[52] H. S. W. Massey and H. B. Gilbody, *Electronic and Ionic Impact*

Phenomena (Oxford University Press, London, 1974), Vol. I, Chap. 1.

[53] D. Voreades, Surf. Sci. **60**, 325 (1976).

[54] R. A. Baragiola, E. V. Alonso, and A. Oliva-Florio, Phys. Rev. B **19**, 121 (1979).

[55] J. Schou, Phys. Rev. B **22**, 2141 (1980).

[56] J. H. Ormrod and H. E. Duckworth, Can. J. Phys. **41**, 1424 (1963).

[57] J. W. Keller, K. W. Ogilvie, J. W. Boring, and R. W. McKemie, Nucl. Instrum. Methods Phys. Res. B **61**, 291 (1991).

[58] G. Schiwietz, J. P. Biersack, D. Schneider, N. Stolterfoht, D. Fink, V. Montemayor, and B. Skogvall, Phys. Rev. A **41**, 6261 (1990).

[59] D. Schneider, G. Schiwietz, and D. DeWitt, Phys. Rev. A **47**, 3945 (1993).

[60] E. V. Alonso, R. A. Baragiola, J. Ferrón, M. M. Jakas, and A. Oliva-Florio, Phys. Rev. B **22**, 80 (1980).

[61] D. Hasselkamp, S. Hippler, A. Scharmann, and T. Schmehl, Ann. Phys. (Leipzig) **42**, 555 (1990).

[62] P. Sigmund, in *Radiation Damage Processes in Materials*, edited by C. H. S. Dupuy (Noordhoff, Leyden, 1975), p. 3.

[63] P. Sigmund and S. Tougaard, in *Inelastic Particle-Surface Collisions*, Springer Series in Chemical Physics 17, edited by E. Taglauer and W. Heiland (Springer-Verlag, Berlin, 1981), p. 2.

[64] M. A. Gruntmann, A. A. Kozochkina, and V. B. Leonas, JETP Lett. **51**, 22 (1990); A. A. Kozochkina, V. B. Leonas, and M. Witte, Nucl. Instrum. Methods Phys. Res. B **62**, 51 (1991).

[65] J. F. Ziegler and J. P. Biersack, TRIM-96, IBM-Research, Yorktown, New York 10598.

[66] J. C. Eckardt, G. Lantschner, N. R. Arista, and R. A. Baragiola, J. Phys. C **21**, L851 (1978).

[67] H. Rothard, C. Caraby, A. Cassimi, B. Gervais, J. P. Grandin, P. Jardin, and M. Jung, Phys. Rev. A **51**, 3066 (1995).

[68] A. Clouvas, H. Rothard, M. Burkhard, K. Kroneberger, C. Bierdermann, J. Kemmler, K. O. Groeneveld, R. Kirsch, P. Misaelides, and A. Katsanos, Phys. Rev. B **39**, 6316 (1989).

[69] K. Bethge and P. Lexa, Br. J. Appl. Phys. **17**, 181 (1966).

[70] P. M. Stier, C. F. Barnett, and G. E. Evans, Phys. Rev. **96**, 973 (1954).

[71] C. F. Barnett and H. K. Reynolds, Phys. Rev. **109**, 355 (1958).